Science of the Total Environment 904 (2023) 166358

Contents lists available at ScienceDirect

Science of the Total Environment

journal homepage: www.elsevier.com/locate/scitotenv

Impacts of leaks and gas accumulation on closed chamber methods for measuring methane and carbon dioxide fluxes from tree stems

Julio A. Salas-Rabaza [a,b], José Luis Andrade [a], Roberth Us-Santamaría [a], Pablo Morales-Rico [c], Gisela Mayora [d], Francisco Javier Aguirre [b], Vicente Fecci-Machuca [b], Eugenia M. Gade-Palma [b], Frederic Thalasso [b,c,*]

[a] Unidad de Recursos Naturales, Centro de Investigación Científica de Yucatán, A.C. (CICY), Calle 43 No. 130, Chuburná de Hidalgo, 97205 Mérida, Mexico
[b] Cape Horn International Center, Universidad de Magallanes, Av. Bulnes 01855, Punta Arenas 6210427, Chile
[c] Departamento de Biotecnología y Bioingeniería, Centro de Investigación y de Estudios Avanzados del Instituto Politécnico Nacional (Cinvestav), Av. IPN 2508, Mexico City 07360, Mexico
[d] Instituto Nacional de Limnología (Inali) Ciudad Universitaria, Colectora Ruta Nac. 168, Paraje El Pozo 3000, Santa Fé, Argentina

HIGHLIGHTS

- CH_4 and CO_2 fluxes from tree stems are significant and important to constrain.
- Stem flux measurements can be affected by leaks and concentration buildup effects.
- We studied these effects in six tree species from two contrasting forest ecosystems.
- These effects led to an underestimation of 40 % for CH_4 and 22 % for CO_2 fluxes.
- A simple method addresses both leaks and concentration buildup effects.

GRAPHICAL ABSTRACT

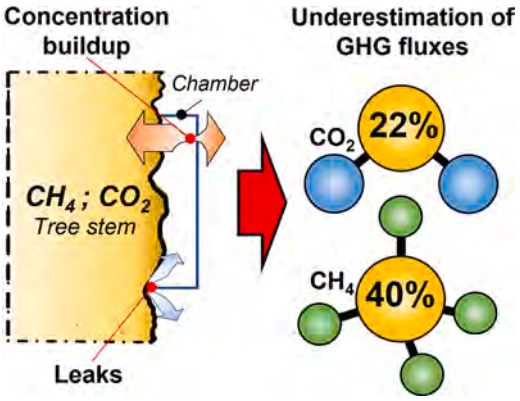

ARTICLE INFO

Editor: Elena Paoletti

Keywords:
Mangrove
Sub-Antarctic
Forest
Greenhouse gas
Bark
Roughness

ABSTRACT

Accurate measurements of methane (CH_4) and carbon dioxide (CO_2) fluxes from tree stems are important for understanding greenhouse gas emissions. Closed chamber methods are commonly employed for this purpose; however, leaks between the chamber and the atmosphere as well as gas accumulation, known as the concentration buildup effect, can impact flux measurements significantly. In this study, we investigated the impacts of concentration buildup and leaks on semi-rigid closed chamber methods. Field measurements were conducted on six tree species, including three species from a Mexican mangrove ecosystem and three species from a Magellanic sub-Antarctic forest. Systematic observations revealed significant leak flow rates, ranging from 0.00 to 465 L h^{-1}, with a median value of 1.25 ± 75.67 L h^{-1}. We tested the efficacy of using cement to reduce leaks, achieving a leak flow rate reduction of 46–98 % without complete elimination. Our study also demonstrates a clear and substantial impact of concentration buildup on CH_4 flux measurements, while CO_2 flux measurements were

* Corresponding author at: Cape Horn International Center, Universidad de Magallanes, Av. Bulnes 01855, Punta Arenas 6210427, Chile.
E-mail address: thalasso@cinvestav.mx (F. Thalasso).

https://doi.org/10.1016/j.scitotenv.2023.166358
Received 27 June 2023; Received in revised form 14 August 2023; Accepted 15 August 2023
Available online 16 August 2023

relatively less affected across all tree species studied. Our results show that the combined effects of leaks and concentration buildup can lead to an underestimation of CH_4 emissions by an average of 40 ± 20 % and CO_2 emissions by 22 ± 22 %, depending on the bark roughness. Based on these findings, we recall a straightforward yet effective method to minimize experimental errors associated with these phenomena, previously established, and reiterated in the current context, for calculating emissions that considers effects of leaks and concentration buildup, while eliminating the need for separate determinations of these phenomena. Overall, the results, combined with a literature review, suggest that our current estimates of GHG flux from tree stems are currently underestimated.

1. Introduction

In the context of climate change, understanding greenhouse gas (GHG) sources and sinks is of paramount importance. Forests are widely acknowledged as global sinks for methane (CH_4; Saunois et al., 2020), where it is produced in the anaerobic deeper soil layer but oxidized in excess, within the aerobic upper layer. However, in flooded forests, like mangroves, water creates an oxygen barrier, turning forest soils into a net CH_4 source. Regardless of the specific forest type, it is well-established that trees play a pivotal role in the transport of CH_4 produced in forest soils (Barba et al., 2019; Covey and Megonigal, 2019). The internal structure of tree stems facilitates the transport of soil CH_4 through both bark aerenchyma and xylem tissues (Teskey et al., 2008; Bloemen et al., 2013; Vroom et al., 2022; Yáñez-Espinosa and Ángeles, 2022).

Tree-mediated emissions, therefore, represent a deviation from the standard CH_4 cycle in forest soils and can offset up to 46.5 % of the soil CH_4 uptake (Machacova et al., 2023). In fact, in the Amazon basin alone, approximately 21.2 ± 2.5 megatons (Mt) of CH_4 are emitted by trees annually, accounting for 10–13 % of global wetland CH_4 emissions (Pangala et al., 2017). On a broader scale, Covey and Megonigal (2019) reported CH_4 emission rates from tree stems ranging from −0.014 to 6.5 g m^{-2} d^{-1}. Regarding carbon dioxide, (CO_2), while forests significantly contribute to carbon dioxide (CO_2) sequestration, capturing about 11 gigatons (Gt) of CO_2 per year (Friedlingstein et al., 2022, emissions from tree stems contribute to 5–38 % of the total ecosystem respiration (Campioli et al., 2016; Yang et al., 2016). Though the contribution of CO_2 emissions from tree stems to the global CO_2 budget is relatively small, it remains relevant for studying tree physiology (Teskey et al., 2017) throughout diurnal and/or seasonal cycles.

Measurement of GHG emissions from tree stems is therefore important, to constrain better our current estimates and to provide better inventories of GHG. Current methods for the determination of these emissions are mostly based on the use of chambers, temporarily fixed on tree stems in which the emitted gases are captured. Among several designs, semirigid chambers, as described by Siegenthaler et al. (2016), are commonly used due to their ease of installation in the field. Regardless of the chamber design, chambers can be operated with continuous (dynamic) or discrete (static) sampling and measurement of the gas concentration. When a detector is used for dynamic measurement, it is usually connected to the chamber through a closed loop, and thus referred to as closed chambers. In that case, fluxes are determined from the derivative of the gas concentration increase within the chamber. The same data processing strategy is generally used when discrete measurements are done.

Whatever the chamber design and the method used, flux measurements are challenging, mostly because they combine low flux magnitude, difficulties in hermetically coupling the chamber and the tree stems, and complex pneumatic behavior of the experimental setup, including the chamber and the pneumatic circuit connecting it to the gas analyzer. One of the challenges in flux measurements is to securely affix the chamber on tree stems avoiding leaks, i.e. gas exchange between the atmosphere and the internal volume of the chamber, that would bias the results. At least in some cases, the shape of tree stems or the natural bark roughness, which is highly variable among species, hinder hermetic sealing, and a common strategy is the use of different sealants (e.g., moldable cement, potting clays, non-caustic silicone, flexible putty adhesive, silicone rubber) to improve chamber's hermeticity (Bréchet et al., 2021; Flanagan et al., 2021; Jeffrey et al., 2021; van Haren et al., 2021). However, the use of sealants is not an absolute guarantee of sealing, at least in the case of very rough bark presenting deep channels, fractures, or irregular shapes. Moreover, even if the chamber is perfectly sealed, leaks might appear in the pneumatic circuit or within the detector, as exemplified by Wilkinson et al. (2018). Leaks from different origins might therefore have a significant impact on the accuracy of emission measurements.

In addition to leaks, another potential challenge, is that during flux measurements an increase in concentration of the measured gases within the chamber is observed. This concentration buildup has the potential to reduce the gas partial pressure gradient between the tree stem and the atmosphere, which would otherwise be observed without a chamber. In turn, this phenomenon may result in underestimated fluxes, as suggested in aquatic ecosystems (Xiao et al., 2016), soils (Welles et al., 2001; Kutzbach et al., 2007; Juszczak, 2013) and observed in trees (Jeffrey et al., 2020; Bréchet et al., 2021; Kohl et al., 2021; van Haren et al., 2021).

Lastly, while this has not been systematically studied, our interpretation is that, in dynamic chambers, the experimental setup forms a complex pneumatic circuit, which can also pose challenges in interpreting the measured concentration profile. Indeed, the gas within the chamber, exhibiting relatively good mixing, is pumped to the analyzer through tubing where plug-flow is observed. Subsequently, the gas passes through the sensor cavity of the analyzer, with its own pneumatic behavior, before returning to the chamber, in the case of closed chambers. In consequence, during the starting period of the measurements, these phenomena can lead to delays, mixing effects, and potential concentration gradients, which hinder the interpretation of the gas concentration profiles observed. These effects have been previously identified and referred to as “dead band” by Siegenthaler et al. (2016) and it is a common practice to discard data from the beginning of the measurements when continuous gas concentration is recorded (Pitz and Megonigal, 2017; van Haren et al., 2021; Epron et al., 2022; Fraser-McDonald et al., 2022).

Overall, the impact of leaks and gas concentration buildup, along with the accurate interpretation of the pneumatic behavior in flux measurement setups, require a systematic and experimental analysis. This is the main objective of the present study. To achieve this goal, we established a mass balance of closed chambers and developed a method to quantify leaks and to analyze the effect of concentration buildup within the chamber headspace, with the hypothesis that by considering and quantifying leaks and analyzing the effect of concentration buildup, the accuracy of greenhouse gas (GHG) flux measurements from tree stems will be improved. The developed method was applied to six different tree species with distinct characteristics, from two contrasting ecosystems: a tropical flooded mangrove in Mexico and a subantarctic non-flooded forest in southern Chile. Through our findings, we quantified the potential errors associated with measuring GHG fluxes from tree stems and discussed various experimental procedures commonly documented in the literature.

2. Materials and methods

2.1. Chamber mass balance

A detailed mass balance of the dynamic closed chamber and the corresponding equations are presented in Supplementary Material (Section S1.1). Briefly, the time derivative of the gas concentration within the chamber (C_C) can be summarized into fluxes from the tree stem and leaks between the atmosphere and the chamber headspace or the pneumatic circuit (Fig. 1).

$$\frac{dC_C}{dt} = F \bullet \frac{A_C}{V_T} + k_L \bullet (C_A - C_C) \quad (1)$$

where F is the observed flux; A_C is the chamber area in contact with the tree stem; V_T, is the total volume of the chamber, the detector and the pneumatic circuit; k_L is the leak constant (h^{-1}), which represents the frequency at which the gaseous content of the chamber and the pneumatic circuit is replaced by external air due to leakage; and C_A is the atmospheric gas concentration, observed during the measurements. It is worth noting that k_L is the ration between the leaks flow rate (Q_L) and V_T. Thus, leaks can be expressed, alternatively, by k_L, or by Q_L.

In Eq. (1), F is the flux measured when the chamber is positioned on the tree stem. Thus, the surface of the bark is exposed to C_C, potentially different from the atmospheric concentration C_A. Hence, the actual flux (F^*), naturally occurring when the bark is exposed to C_A (no chamber) might be different from F. Since mass transfer is a lineal function of the concentration gradient, we can estimate that the measured flux is a function of the ration between the concentration gradient with and without a chamber:

$$F = F^* \bullet \frac{(C_i - C_C)}{(C_i - C_A)} \quad (2)$$

where (C_i-C_C) and (C_i-C_A) are the concentration gradient observed during the chamber measurement and the gradient that would be otherwise observed in the absence of a chamber, respectively. Hereafter, Eq. (2) will be referred to as "the concentration buildup effect", which bears similarity to equations commonly used in the study of aquatic ecosystems (Xiao et al., 2016) and wetlands (Kutzbach et al., 2007; Juszczak, 2013). Therefore, considering this concentration buildup effect, Eq. (1) becomes:

$$\frac{dC_C}{dt} = F^* \bullet \frac{(C_i - C_C)}{(C_i - C_A)} \bullet \frac{A_C}{V_T} + k_L \bullet (C_A - C_C) \quad (3)$$

It is worth noting that, in an ideal case, at the onset of the measurement, just after chamber installation, C_C might be equal to C_A, and Eq. (3) is greatly simplified, as follows:

$$\frac{dC_C}{dt} = F^* \bullet \frac{A_C}{V_T} \quad (4)$$

Eq. (4) holds significant importance as it suggests that accurately measuring flux, free from the effects of leaks and concentration buildup, can be achieved by analyzing the initial slope of gas concentration within the chamber (Eq. (4)). However, in practice, measuring this initial slope, when C_C equals C_A, presents challenges for two primary reasons. Firstly, at the start of the measurement, there may be differences in gas concentration among the chamber, the pneumatic circuit, and the detector, leading to a transient period as the system begins to operate. This is the main reason why it is a common practice to disregard data from the beginning of the measurements when calculating fluxes using continuous sampling (Siegenthaler et al., 2016; Pitz and Megonigal, 2017). Secondly, during the installation of the chamber, gases may already accumulate within it or be influenced by the proximity of operators (often notable with CO_2 expelled by the operators), resulting in C_C being higher than C_A. Consequently, in real-case scenarios, even at the onset of the measurements, C_C often exceeds C_A and the observed concentration increase is influenced by multiple mechanisms beyond just the flux. Under these conditions, Eq. (4) becomes inappropriate, and ideally, Eq. (3) should be employed to accurately quantify the flux.

In Eq. (3), if the time interval dt is sufficiently small, we can estimate the change in C_C over time ($C_{C,t}$), after the chamber has been installed and operated, by adding the rate of change (dC_C/dt) multiplied by the small-time interval (Δt) to the previous value of C_C ($C_{C,t-1}$). Mathematically, this approximation can be expressed as follows:

$$C_{C,t} = C_{C,t-1} + \left(F^* \bullet \frac{(C_i - C_{C,t-1})}{(C_i - C_A)} \bullet \frac{A_C}{V_T} + k_L \bullet \left(C_A - C_{C,t-1}\right) \right) \bullet \Delta t \quad (5)$$

In Eq. (5), the geometry of the chamber (A_C, V_T) is known, and C_A can be readily measured in the field. Therefore, if k_L is known, by calibrating Eq. (5) to the experimental C_C time series, it becomes possible to determine F^* and C_i, effectively accounting for the effects of leaks and concentration buildup.

For the determination of k_L, we developed a method, that is described in detail in the Supplementary Material (Section S1.2). Briefly, the method involves inducing a transient state by injecting a pulse of CH_4 into the chamber, artificially creating a relatively high concentration of CH_4. Following this injection, any leakage would result in an asymptotic decrease in the CH_4 concentration, until the system reaches a new steady state. Assuming a well-mixed behavior of the gas phase within the chamber, this asymptotic decrease could be described by Eq. (6), where $C_{C,0}$ and $C_{C,f}$ are the CH_4 chamber concentration at time zero (shortly after pulse injection) and after the chamber reaches steady state (details provided in Section S1.2).

$$C_{C,t} = C_{C,0} + \left(C_{C,0} - C_{C,f}\right) \bullet \left(1 - exp(-k_L \bullet t)\right) \quad (6)$$

By calibrating Eq. (6) to the experimental C_C time series, it is possible to determine $C_{C,f}$ and k_L, with the latter being the parameter of primary interest. However, it is important to note that for this purpose, $C_{C,0}$ must be sufficiently high, typically a few hundreds of ppm, to ensure a subsequent decrease in $C_{C,t}$ over time. Furthermore, in the Supplementary Material, we demonstrate that while Eq. (6) is correct, it does not fully capture the intricate pneumatic behavior observed in certain cases (Fig. S2). Although we have mathematically described this complex behavior, it falls outside the primary scope of the present study, which is centered around evaluating the impact of leaks on emissions. Therefore, we have included these findings in the Supplementary Material, Section S1, provided for those readers who are interested in exploring this aspect further.

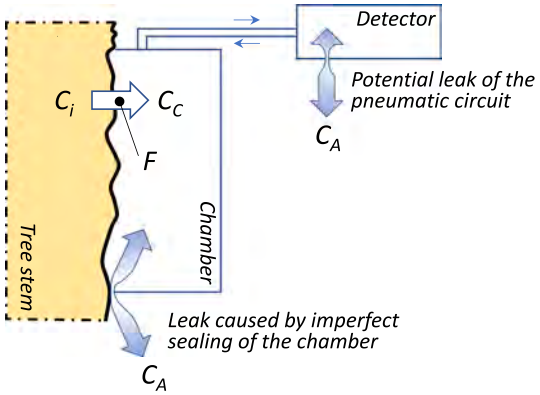

Fig. 1. Conceptual scheme of the chamber mass balance. Where F is the flux from the tree stem, and C_C, C_A and C_i are the gas concentration within the chamber, the atmospheric gas concentration, and the tree internal gas concentration, respectively.

2.2. Fluxes, leaks and C_i determination

In the present work, fluxes of CH_4 and CO_2 (F^*_{CH4}, and F^*_{CO2}, respectively), were determined according to the following 4-step protocol (materials being described in Section 2.3). Step 1, semi-rigid chambers were tidily fixed on the tree stem using 3 to 4 nylon straps. Step 2, the air content of the chamber where CH_4 or CO_2 potentially accumulated during chamber installation, was replaced by fresh ambient air over 2 min, with a portable external air pump (Flextailgear Tiny Pump, Mexico). Step 3, the chamber was immediately connected, in a closed loop, to a laser ultraportable greenhouse analyzer (i.e. UGGA, model 915–0011-1000, Los Gatos Research, ABB, USA). Step 4, the CH_4 and CO_2 concentration within the chamber was measured for 10–15 min. Step 5, k_L was determined from the injection of 1 mL of CH_4 into the chamber. Pulse injection and k_L determination was done after flux measurement, to avoid any potential effect of increasing artificially CH_4 concentration to much higher levels than standardly observed during flux determination. Specifically, k_L was determined from Eq. (6) calibration (details provided in Section S1.2). Step 6, C_C dataset measured during step 4, was used to calibrate Eq. (5), which was adjusted to the experimental data, using Ci and F^* as adjustment parameters, and where k_L was determined during step 5.

2.3. Experimental setup

Depending on the size of the tree, we used four different sizes of semi-rigid chambers (#1, 0.50 × 0.30; #2, 0.30 × 0.24; #3 0.24 × 0.18; #4, 0.15 × 0.10 m), all of them composed of a 0.7 mm thick impermeable polyethylene terephthalate (PET) plastic sheet glued along its entire perimeter to a 20 × 30 mm closed cell neoprene foam (Seals+Direct Ltd., Hamphshire, UK), as described in Siegenthaler et al. (2016). The distance between the tree stem and the PET plastic sheet, which determined the chamber volume, was 20 mm. The chambers were connected in a closed loop to the UGGA, with two 6 mm external diameter (4 mm internal diameter) flexible polyurethane tubing (PUN-6X1-DUO-BS, Festo, Mexico). To reduce the volume of the pneumatic circuit and improve the recirculation rate between the chamber and the detector, the length of this tubing was as short as possible (about 2 m) in dry ecosystems, but of up to 12 m long in the mangrove ecosystem, to ensure that the detector was placed in a dry and safe place. It should be noted that, in contrast to the relatively heavy UGGA model used in the present work (16 kg plus batteries), the current trend is towards lightweight and backpack portable GHG detectors, making their deployment in close vicinity of the chamber easier. The volume of the semi-rigid chambers used is an important parameter, which is required for flux determination (Eq. (3)). Compared to rigid chamber, which have an approximately constant volume, the volume of semi-rigid chambers depends on the deformation of the chamber around the tree stem. The volume of the chambers was determined according to Siegenthaler et al. (2016), and ranged 0.22–2.9 L. On the contrary to several previous reports, in the present work, the relatively low thickness of the chambers used impeded the use of an internal fan to homogenize the chamber headspace. However, the relatively small chamber volume and the UGGA flow rate (1.2 L min^{-1}) ensured a relatively good mixing of the chamber volume. In some experiments, the impact of moldable cements (Play-Doh, purchased in toy stores, México) was used as leak repressor. In each case, flux and leak measurements were done according to the standard method described above.

2.4. Sites description and campaigns

The method was applied to two contrasting forest ecosystems; a mangrove forest located in Celestun, in the Yucatan Peninsula (Mexico; 20.855, −90.374) and a sub-Antarctic forest located in Puerto Williams, in the Navarino Island (Chile; −54.949, −67.660). Celestun is characterized by a hot and semi-arid climate with a marked rainfall season (Orellana et al., 2010), an annual mean rainfall of 746.7 mm (mean monthly range from 8.2 to 144.0 mm) and an annual mean temperature of 26.4 °C (mean monthly range from 23.2 to 28.5 °C) (CONAGUA, 2023). In turn, Puerto Williams has a tundra and oceanic climate with an annual mean rainfall of 822 mm (mean monthly range from 51 to 131 mm) and an annual mean temperature of 6.1 °C (mean monthly range from −2.8 to 7.2 °C) (Aguirre et al., 2021; DMC, 2023). In the mangrove ecosystem, we measured flux and leaks on the stem of the tree dominant species; "red mangrove" (Rm; *Rhizophora mangle*), "black mangrove" (Ag; *Avicennia germinans*), and "white mangrove" (Lr; *Laguncularia racemosa*). In Navarino Island, we also characterized the three dominant species; "low deciduous beech" (Na; *Nothofagus antarctica*), "high deciduous beech" (Np; *Nothofagus pumilio*), and "evergreen beech" (Nb; *Nothofagus betuloides*). It is worth mentioning that, in each ecosystem, the bark of the trees was drastically different among species (Figs. S3 and S4), offering a good model to evaluate the impact of leaks. For each species, nine to thirteen trees were selected with a range of diameter at breast height (DBH) from 3.8 to 56.6 cm. Then flux, leaks and bark roughness were determined in each tree at two stem heights, at 0.25 m and 1.4 m (up to 26 measurements by species). In the case of Rm, characterized by stilt roots, all measurements were made at 0.25 m above the last stilt root. According to the stem diameter, chambers #1 and #2 were used for larger diameters mostly at a tree height of 0.25 m, chambers #2 or #3 were used for medium diameters at both tree heights, and chambers #3 and #4 were used for smaller diameters (see Table S2 for further details). The diameter of the trees was measured using a sewing measuring tape (Singer 50,003 ProSeries) which was calibrated with a caliper (Mitutoyo 530–101). As the objective of the present work was to quantify leaks and the effects of concentration buildup, rather than focusing on reporting emissions, we determined fluxes during the daytime only, typically from 10 am to 4 pm. The field campaign in México took place from September 6th to September 18th, 2021, while the Navarino campaign took place from February 20th to March 3rd, 2022. During these campaigns, the mean temperature was 30.5 ± 2.0 °C and 8.9 ± 3.1 °C for Celestun and Puerto Williams, respectively. While the mean wind speed was 1.2 ± 0.5 km h^{-1} and 6.8 ± 4.5 km h^{-1} for Celestun and Puerto Williams, respectively. Weather data were obtained from public data of nearby stations, namely, from the Celestun weather station (#31040; CONAGUA, 2023) located 2800 m west of the mangrove location, and from Puerto Williams airport station (#550001; DMC, 2023), located 3200 m northeast from the forest where measurements were taken.

2.5. Bark roughness determination

In order to correlate leaks to bark roughness, which is on first approximation a governing parameter of leaks, we developed our own method, founded on our field experience. The method is based on a 0.2 m contour gauge (6″ Contour Gauge, General Tools & Instruments, Mexico) that was firmly pressed against the tree bark at the same height where chamber was placed. We defined bark roughness (R; Fig. 2) as the relative difference between the length of the bark contour (L') and its equivalent smooth length (L; Eq. (7)). In each case, L' was determined from a scaled photograph of the gauge taken in the field, and analyzed with ImageJ (Schneider et al., 2012).

$$R = \frac{(L' - L)}{L} \bullet 100 \tag{7}$$

Since the bark geometry of the tree stems differs along both axes, we distinguished axial and radial roughness, as follows. Axial roughness ($R_{A\%}$) was defined as illustrated in Fig. 2A and Eq. (8):

$$R_{A\%} = \frac{(L'_A - L_A)}{L_A} \bullet 100 \tag{8}$$

In turn, radial roughness ($R_{R\%}$) was defined as the perimeter section

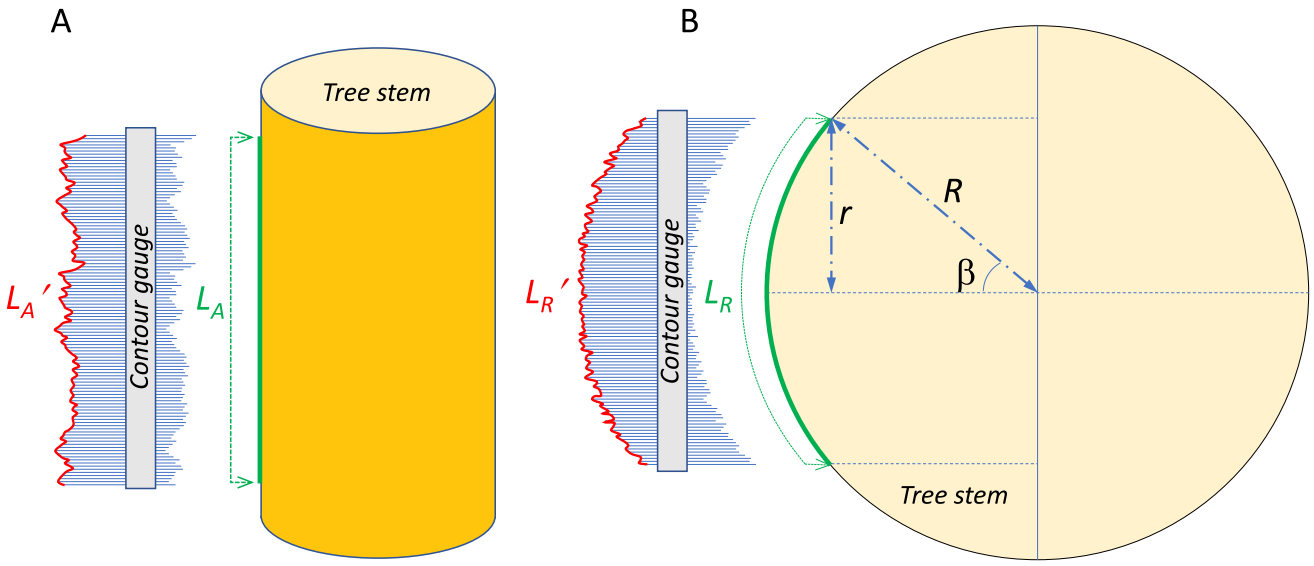

Fig. 2. Conceptual scheme of bark roughness for both axial (A) and radial (B) determination in a longitudinal and cross sections, respectively.

of the bark contour (L'_R) and the section of a smooth circle of the same tree radius (L_R), as shown in Eq. (9) and Fig. 2B.

$$R_{R\%} = \frac{(L'_R - L_R)}{L_R} \bullet 100 \tag{9}$$

In Eq. (9), L_R can be determined, as follows, where angles are expressed in radians and where r is half the length of the contour gauge;

$$L_R = \frac{2\beta}{2\pi} \bullet 2\pi R = 2\beta R \tag{10}$$

$$Sin(\beta) = \frac{r}{R}; \beta = arcsin\left(\frac{r}{R}\right) \tag{11}$$

$$L_R = 2 \bullet R \bullet arcsin\left(\frac{r}{R}\right) \tag{12}$$

For each measurement, $R_{A\%}$ was taken from both lateral sides of the chamber and $R_{R\%}$ was taken from upper and lower sides of the chamber. For each position, a single mean bark roughness percentage ($R_{\%}$) was determined, using a weighted average (Eq. (13)), where H_C and W_C are the height and width of the chamber used.

$$R_{\%} = \frac{R_{A\%} \bullet H_C + R_{R\%} \bullet W_C}{H_C + W_C} \tag{13}$$

2.6. Data treatment and statistics

Eqs. (5) and (S8) were calibrated to experimental data using a Generalized Reduced Gradient (GRG) non-linear tool and minimizing the root-mean-square error (RMSE) between experimental data and models. Normality (Shapiro-Wilk) and homoscedasticity (Levene) were tested prior to statistical analysis. Then, two-way ANOVA were performed. Most variables had a positive skew, which were log-transformed to achieve normality. If normality was not achieved, then a Kruskal-Wallis test was applied instead. Statistical differences among tree species, chamber designs, and ecosystems, were determined according to Tukey's post-hoc tests. All statistical analysis were performed in R language version 2023.03.1.446 (Posit Team, 2023) or with Origin(Pro) software (OriginLab Corporation, 2016). In the present work, results are usually presented in term of the median ± one standard deviation, unless specified. Boxplots in Section 3 and Supplementary Material display the first quartile (Q1), median (Q2), and third quartile (Q3) as boxes, with whiskers extending to the minimum and maximum values. Outliers are represented as individual data points beyond the whiskers.

3. Results and discussion

3.1. Leaks characterization

Fluxes and leaks were determined 153 times in different trees and under different configurations. Overall k_L ranged 0.00–284 h^{-1}, with a median of 1.25 ± 46.9 h^{-1}, which corresponded to leaks flow rates (Q_L) from 0.00 to 465 L h^{-1}, with a median of 1.25 ± 75.67 L h^{-1}. Thus, the chambers were far from being well sealed, and significant gas exchanges occurred between the chamber headspaces and the atmosphere. It is worth noting that the leak flow rates reported here are not exclusively caused by the chamber sealing, but include all components of the measurement setup, including the UGGA leak flow rate of 0.27 ± 0.05 L h^{-1}, reported in Section S1.3. Compared to the total leak flow rate, the UGGA's leak represented, on average, about 8.8 % of the total leaks.

No significant difference of leaks was observed among tree species, except Na, which were significantly higher than those observed with Rm, Ag, Lr, and Np ($P < 0.05$; Fig. 3A). The notable difference in leaks between Na and the other tested species was most certainly due to bark roughness, as $R_{\%}$ of Na (51.1 ± 16.8 %) was significantly higher than all other species ($P < 0.05$; Fig. S4). It is important to mention that there were no differences between the roughness measured at two stem heights within each species (Table S1). To further characterize possible correlations between bark roughness and leaks, $R_{\%}$ of the measured trees was compared to k_L. A positive exponential correlation was observed between $R_{\%}$ and k_L ($P < 0.05$: Fig. S5). On the contrary, no significant difference was observed among k_L measured in the same trees, but with different chambers ($p = 0.66$), which is not surprising because k_L is a specific parameter, i.e. where Q_L is proportional to V_T, (Fig. S6).

Leaks between the chamber and the atmosphere might be dependent on the weather conditions, and particularly on the wind speed, which might alter the gas exchange between the chamber and the atmosphere, leading to flux measurement errors or artifacts (Bain et al., 2005; Maier et al., 2019; Jiang et al., 2023). To check for the latter, in another set of experiments, 6 replicates of k_L, were determined over two hours, in two trees; one presenting a moderate roughness (Np; $R_{\%} = 4.10$) and one presenting a high roughness (Na; $R_{\%} = 88.58$). This test was done on a day with variable winds, i.e., 18.7 ± 6.0 km h^{-1} with gusts at 39 km h^{-1}. In the case of Np, the mean k_L was equal to 0.86 ± 0.02 h^{-1}, with a coefficient of variation of 2.0 %, which suggest that the variable wind had little effects on leak determination. This was confirmed by a generally good adjustment of the leak model (Eq. (S8)) to the experimental data, with a mean R^2 of 0.999 ± 0.001. On the contrary, in the

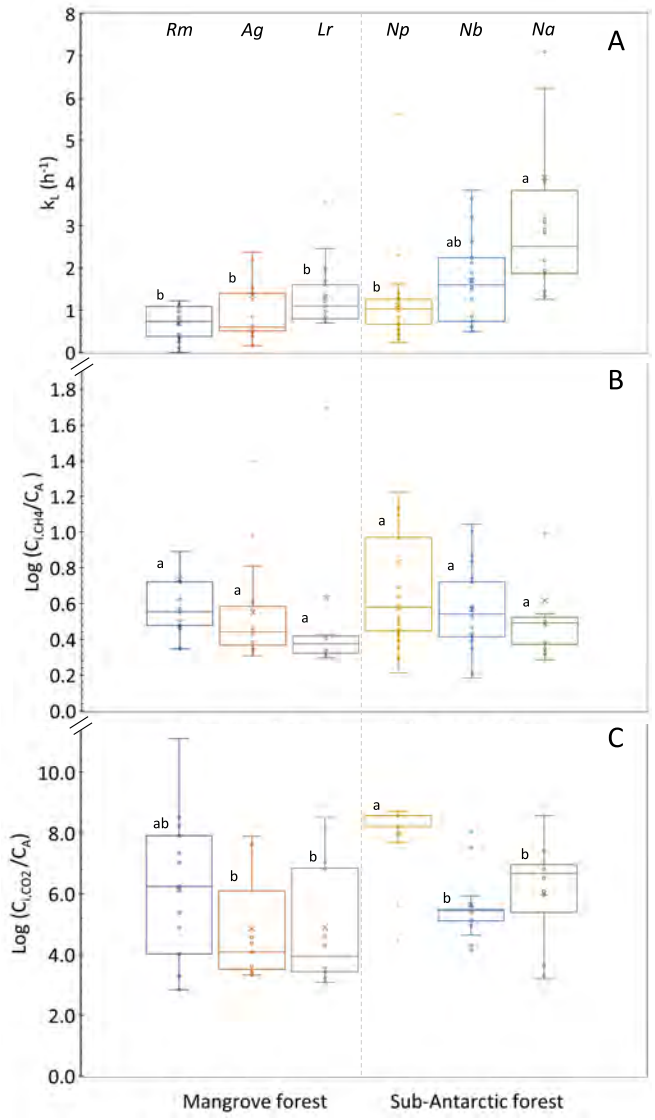

Fig. 3. Leaks, expressed as k_L, among the different tree species (A); ratio between C_i and C_A, for CH_4 (B) and CO_2 (C).

case of Na, the mean k_L was 16.8 ± 6.2 h^{-1} (coefficient of variation of 37 %), and with a poorer model fitting (R^2 of 0.951 ± 0.109). Therefore, the wind conditions had a major impact on leak detection in the tree with high roughness, and it would be advisable, in these cases, to determine fluxes during stable and moderate wind conditions or to use cement to reduce k_L.

3.2. Impact of moldable cement

The most common strategy to avoid or reduce leaks is using cement. To evaluate the impact of cement, another set of measurements was done with and without moldable cement on trees where significant leaks were previously detected. Overall, the use of cement reduced the leak flow rates by 46–98 %, with a mean of 92 ± 20 % (n = 20), which corresponded to a reduction of k_L by 92 ± 27 %. Thus, leaks were not completely avoided by cement, but they were reduced to a large extent (data not shown).

3.3. Fluxes and C_i determination

As expected from Eq. (5), an asymptotic trend of C_C was almost systematically observed, more clearly marked for $C_{C,CH4}$ than for $C_{C,CO2}$, as exemplified on Fig. 4. Notably, at the onset of the measurements, and despite the chamber ventilation performed to allow for equilibration of the experimental setup, an instability that lasted 2–3 min was standardly observed (Fig. 4). Therefore, calibration of Eq. (5) was done discarding this initial period. Overall, F^*_{CH4} ranged 0–2.05 mg m^{-2} h^{-1} with a mean of 0.17 ± 0.29 mg m^{-2} h^{-1}. These emissions are in accordance with the literature, i.e. −0.06 to 271.68 mg m^{-2} h^{-1} (Covey and Megonigal, 2019), with an estimated mean from these reported values of 22.16 ± 53.40 mg m^{-2} h^{-1}. Regarding CO_2, F^*_{CO2} ranged 32–2851 mg m^{-2} h^{-1} with a mean of 358 ± 378 mg m^{-2} h^{-1}. This range of F_{CO2} range is also in accordance with the literature, i.e. 0.33 to 406.05 mg m^{-2} h^{-1} (Campioli et al., 2016; Yang et al., 2016; Salomón et al., 2017), with an estimated mean from these reported values of 112.55 ± 100.38 mg m^{-2} h^{-1}. In the case of mangrove trees, the mean stem CH_4 flux was 0.10 ± 0.17 mg m^{-2} h^{-1}, which is slightly greater than the mean stem CH_4 flux of 0.04 ± 0.05 mg m^{-2} h^{-1} previously reported for mangroves of the same genera (He et al., 2019; Jeffrey et al., 2019; Zhang et al., 2019; Dušek et al., 2021; Gao et al., 2021). Concerning the *Nothofagus* species measured on Navarino Island, the mean stem CH_4 flux was 0.06 ± 0.15 mg m^{-2} h^{-1}, with no previous reports yet.

By model calibration, we observed that $C_{i,CH4}$ was varying largely and was relatively close to the atmospheric concentration. To reflect the latter more evidently, we expressed the closeness of C_i to C_A by the ratio between them. The $C_{i,CH4}/C_{A,CH4}$ ratio was 3.2 ± 11.5 (median ± one standard deviation; Fig. 3B). The latter indicate that the CH_4 fluxes measured were highly sensitive to the concentration buildup phenomenon, and that this observed behavior was shared by the six tested tree species, with no significant difference (Fig. 3B). The same approach with CO_2 provided a very distinct behavior, with a median $C_{i,CO2}/C_{A,CO2}$ ration of 337 × 10^3 ± 19 × 10^3 (Fig. 3C), suggesting that, in most cases, no significant effect of CO_2 concentration buildup within the chamber was observed. Although Np was characterized by a $C_{i,CO2}$ significantly higher than those of the other tree species, all species exhibited a $C_{i,CO2}/C_{A,CO2}$ several order of magnitude above $C_{i,CH4}/C_{A,CH4}$ (Fig. 3B and C).

To further visualize the segregated impact of leaks and concentration buildup during flux measurements, Fig. 5 shows the CH_4 and CO_2 concentration profiles in a chamber, established numerically, from the mean results obtained in the present work, i.e. median A_C, V_T, F^*, k_L and C_i. It can be observed that, compared to the linear increase of C_C expected in an ideal system, the presence of leaks and the effects of concentration buildup, whether separately or combined, resulted in a similar curvature in the C_C trends. However, the contribution of both effects is drastically different among CH_4 and CO_2 trends. In the case of CH_4, most of the curvature effect is caused by the concentration buildup, while in the case of CO_2, the effect of C_i appears insignificant. Overall, 76 % of the deviation from linear $C_{C,CH4}$ increase was explained by the

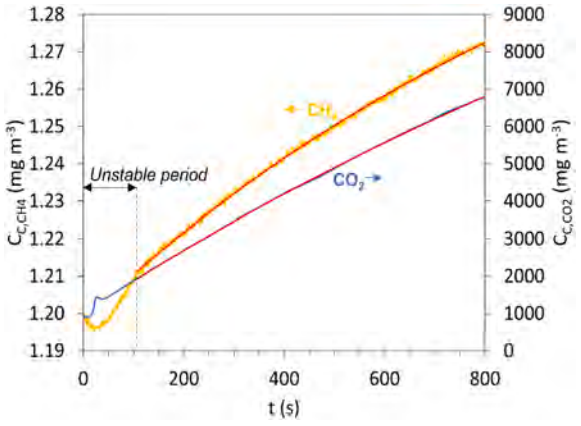

Fig. 4. Example of C_C measurement and model fitting (Eq. (5); red continuous lines).

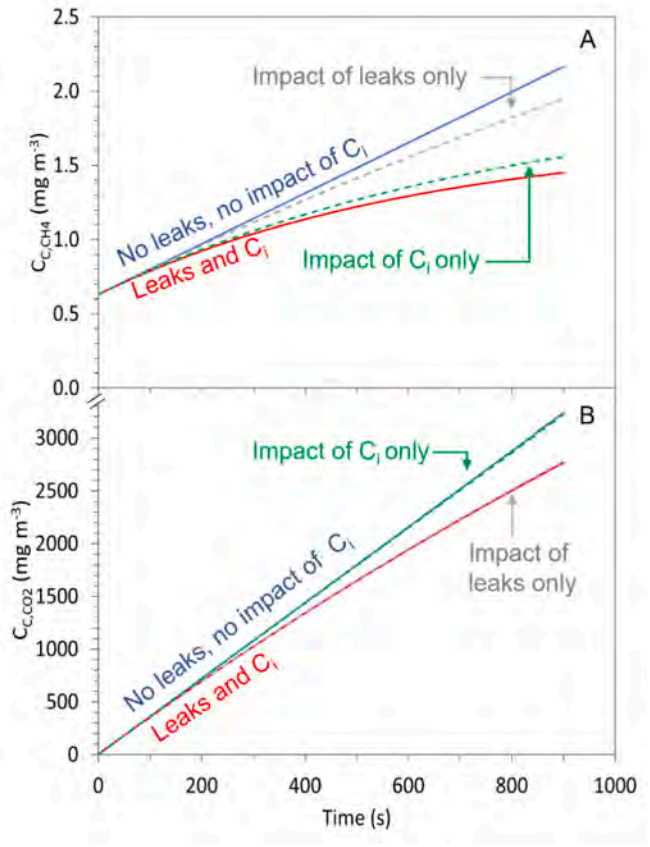

Fig. 5. Theoretical profiles of $C_{C,CH4}$ (A) and $C_{C,CO2}$ (B) that are expected during chamber deployment, from median A_C, V_T, F^*, k_L and C_i, without considering leaks and the effect of C_i (ideal and linear profile), considering the effect of leaks only (median k_L), considering only the concentration buildup (median C_i), and considering both median k_L and C_i.

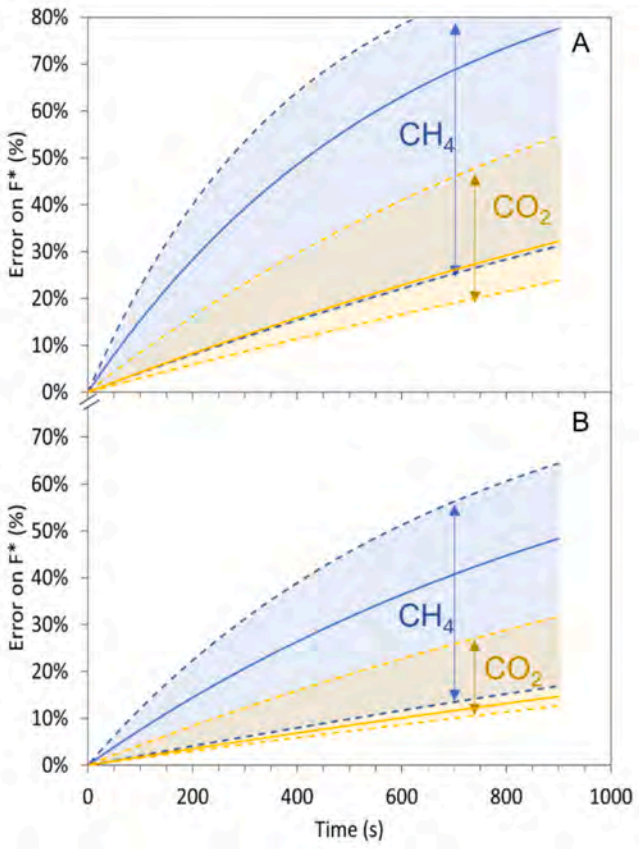

Fig. 6. Range of error theoretically committed when discarding delay in starting measurements of C_C (A) and as a function of the duration of the measurements (B), for CH_4 (light blue area) and for CO_2 (light yellow area). Continuous lines show the error considering the median k_L, F^*, and C_i data observed in the present work, while dashed lines shows the limit between the second and third quartile of these parameters.

effect of concentration buildup, and 24 % was explained by leaks. The same exercise for CO_2, indicated that 3 % of the deviation to the linear $C_{C,CO2}$ increase was explained by the effect of concentration buildup, and 97 % was explained by leaks (k_L). Therefore, the relative weight of both mechanisms is drastically different among gases.

3.4. Errors in F determination

At the beginning of the measurements, when the chamber has been properly ventilated with atmospheric air and if C_C is equal to C_A, the initial slope of C_C accurately reflects the actual flux, independent of k_L and C_i. Therefore, one common error in determining F would be to assume that the initial linear slope is correct, because independent of leaks and concentration buildup effects. This would be an error, because disregarding potential gas accumulation during chamber installation or any other influences in the early stages of measurement. To estimate this potential error, we conducted a numerical analysis to determine the range of errors in flux determination, considering a delay between the start of chamber operation ($t = 0$, C_C equals C_A) and the actual acquisition of C_C data. In this exercise, we focused exclusively on the effect of gas accumulation resulting from tree emissions during chamber deployment, as other potential effects are stochastic and challenging to quantify. Based on the mean, second, and third quartiles of k_L, F^*, and C_i complete dataset, we compared the slope of C_C observed after a delay time with the theoretical slope at time zero (Eq. (3)). Fig. 6A shows that even a short delay of three minutes can result in an underestimation ranging 7–37 % in F_{CH4} determination and 5–15 % in F_{CO2} determination.

A second, more obvious error in determining F^* would be to neglect the effects of leaks and concentration buildup and to assume that the slope between the initial C_C value and C_C at any time adequately reflects the flux. This error would occur when using a discrete sampling strategy or employing linear regression for dynamic C_C measurements. To assess the magnitude of this error, in this case too, we calculated the error range using the second and third quartiles of our complete dataset of k_L, F^*, and C_i. The results (Fig. 6B) are that, for instance, a short 3-min measurement would result in an underestimation ranging from 4 to 20 % for F_{CH4} and from 3 to 8 % for F_{CO2} determination. It is important to note that the error presented in Fig. 6B does not account for the delay-induced error shown in Fig. 6A, which further emphasizes the magnitude of errors, when combined. Moreover, Fig. 6B highlights that the errors resulting from discrete measurements over extended durations reach magnitudes that potentially exceed an acceptable threshold. For instance, a 15-min measurement may result in a range of underestimation from 17 % to 64 % for F^*_{CH4}, not to mention the potential errors when there are several hours between measurements, as sometimes reported.

To estimate the experimental error, combining the errors caused by delay and experimental duration, we determined fluxes in each C_C profile measured in the present work, discarding effects of leaks and concentration buildup, and considering in each case only the first three minutes of measurement, after the initial instable period. Under these conditions, the error committed on F^*_{CH4} was an underestimation by 1.3–92 % with a median of 40 ± 20 %, and an underestimation by 0–91 % with a median of 22 ± 22 %, regarding F^*_{CO2}, similar to the 33 %

underestimation in CH_4 fluxes from soils found by Pihlatie et al. (2013) in static chambers.

3.5. Practical considerations

The chamber model and the results obtained indicate that leaks and concentration buildup during flux measurements have an important impact on the estimation of greenhouse gas (GHG) emissions from tree stems. Leaks are difficult to eradicate, even when using moldable cement, and the effects of concentration gradients are highly variable among gases. Based on this analysis, it is advisable to consider both phenomena. However, this implies determining k_L and C_i, which would require relatively long and tedious fieldwork. However, the determination of leaks and C_i, as performed in the present study for explanatory purposes, is not mandatory. Data can be corrected using a simple analytical solution previously suggested (see below), although it is not commonly employed.

During the deployment of the chamber, it is observed that the concentration of C_C follows an asymptotic curve from an initial value $C_{C,1}$ to a final value $C_{C,2}$, as the chamber reaches a steady-state condition and C_C becomes independent of time, as discussed by Welles et al. (2001) for soil CO_2 fluxes. This concentration trend can be described by a standard exponential equation that has been previously described by several authors (Hutchinson and Mosier, 1981; Pedersen et al., 2010; Pihlatie et al., 2013), similar to Eq. (6) (Eq. (14); specific details provided in Section S1.4).

$$C_{C,t} = C_{C,2} - \left(C_{C,2} - C_{C,1}\right) \bullet exp(-k_t \bullet t) \tag{14}$$

where k_t is a kinetic constant which include all kinetic parameters of flux and leaks. Eq. (14) is numerically equivalent to Eq. (5), and can be used instead, without requiring the determination of k_L and C_i. Eq. (14) can be easily calibrated using any experimental C_C segment of the measurement series, using $C_{C,2}$ and kt as adjustment parameters. After determining these parameters, F^* can be numerically determined, assuming $C_C = C_A$, as follows:

$$F^* = \left(\frac{dC_C}{dt}\right)_{t=0} \bullet \frac{V_T}{A_C} = k_t \bullet \left(C_{C,2} - C_A\right) \bullet \frac{V_T}{A_C} \tag{15}$$

Eq. (15), can be used in all cases, in substitution to Eq. (5), without requiring the identification of k_L and C_i.

Regarding the implications of our findings on the methods used for the determination of GHG emissions from tree stems, the dynamic closed chamber, i.e., continuous measurement of C_C in a closed chamber, is certainly the best method, as it would allow calibration of Eq. (14) with a large dataset. Discrete sampling in a closed chamber (static chamber method) could also be applied using this approach, but only if several samples are taken, to allow for Eq. (14) calibration.

In all cases, it is highly advisable to proceed to a good ventilation of the chamber prior to any measurement (Hutchinson and Livingston, 2001), in order to reach initial condition where C_C is as close as possible to C_A. The results obtained in the present work and the experimental strategy suggested indicate that the use of cement is not a requirement, although it would certainly provide better data quality in trees with severe roughness, i.e., reducing experimental noise. It is also advisable, in order to reduce noise at the onset of measurements, to use a pneumatic circuit as short as possible by placing the detector as close as possible to the chamber and to consider detectors with an internal pump flow rate as high as possible or even to consider an additional external recirculation pump. These recommendations are favorable to a short gas residence time within the pneumatic circuit, thus allowing a rapid equilibration between the chamber and the detector, producing better data quality at the onset of the measurement.

4. Conclusion

The effects of leaks and of concentration buildup severely impair flux measurements from tree stems and must be considered. After conducting a comprehensive literature review on CH_4 fluxes from tree stems over the past decade (69 items, Table S3), we observed that linear adjustment was consistently used in 75 % of the reports, while the choice of asymptotic-like data adjustment for flux calculation was only utilized in approximately 9 % of the cases. Consequently, the use of asymptotic fitting is not a common practice and remains limited, despite its ability to effectively handle data with or without significant curvature. Additionally, among the reports that employed linear adjustment, 42 % were based on discrete sampling methods, which complicates the accurate determination of potential data curvature over time caused by leaks and/or concentration buildup. By separately analyzing the impacts of leaks and concentration buildup, our study underscores the importance of both factors in accurately measuring CH_4 fluxes, and leaks having a dominant effect on CO_2 flux determination. Overall, this study serves as a reminder of the key findings highlighted in previous reports: the precise assessment of greenhouse gas emissions from tree stems necessitates the consideration of both leaks and concentration buildup, with the utilization of asymptotic data adjustment methods. These results, combined with the literature review, also suggest that our current estimates of GHG flux from tree stems are currently underestimated.

CRediT authorship contribution statement

Julio A. Salas-Rabaza: Conceptualization, Funding and administrative management, Field/lab work México/Chile, Data processing, Writing - Original draft preparation; José Luis Andrade: Funding and administrative management, Revision - Original draft; Roberth Us-Santamaría: Fieldwork and logistic Mexico; Pablo Morales-Rico: Fieldwork Mexico, Gisela Mayora: Fieldwork Mexico; Francisco Javier Aguirre: Fieldwork and logistic Chile; Vicente Fecci-Machuca Field/lab work Chile; Eugenia M. Gade-Palma: Fieldwork Chile; Frederic Thalasso: Conceptualization, Funding and administrative management, Field/lab work México/Chile, Data processing, Writing - original draft preparation.

Declaration of competing interest

The authors declare that they have no known competing financial interests or personal relationships that could have appeared to influence the work reported in this paper.

Data availability

Data will be made available on request.

Acknowledgements

We thank the “Consejo Nacional de Ciencia y Tecnología (CONACYT)” for the financial support received (project A3-S-75824), as well as for the support to Julio A. Salas-Rabaza and Pablo Morales-Rico (grants #760092 and #703565, respectively). Julio A. Salas-Rabaza also thanks to the International Tropical Timber Organization (ITTO) Fellowship's reference number 050/20A. Gisela Mayora, acknowledge the financial support (RESOL-2021-973-APN-DIR#CONICET) from the “Consejo Nacional de Investigaciones Científicas y Técnicas” (CONICET). Frederic Thalasso and Julio A. Salas-Rabaza received a partial financial support from the Cape Horn International Center project (ANID, CHIC-FB210018). Authors thank M.Sc. Victoria Teresita Velázquez Martínez, M.Sc. Francisco Silva-Olmedo, M.Sc. Gabriela Cerón-Aguilera, Geophysicist Matías Troncoso, and Ph.D. Brenda Riquelme for their technical support. The authors declare that they have no conflict of interest.

Appendix A. Supplementary data

Supplementary data to this article can be found online at https://doi.org/10.1016/j.scitotenv.2023.166358.

References

Aguirre, F.J., Squeo, F.A., López, D., Ramiro, D., Buma, B., Carvajal, D., Jaña, R., Casassa, G., Rozzi, R., 2021. Gradientes climáticos y su alta influencia en los ecosistemas terrestres de la Reserva de la Biosfera Cabo de Hornos. Anales Instituto de la Patagonia, Chile. https://doi.org/10.22352/AIP202149012.

Bain, W.G., Hutrya, L., Patterson, D.C., Bright, A.V., Daube, B.C., Munger, J.W., Wofsy, S. C., 2005. Wind-induced error in the measurement of soil respiration using closed dynamic chambers. Agric. For. Meteorol. 131 (3–4), 225–232. https://doi.org/10.1016/j.agrformet.2005.06.004.

Barba, J., Bradford, M.A., Brewer, P.E., Bruhn, D., Covey, K., van Haren, J., Megonigal, J. P., Mikkelsen, T.N., Pangala, S.R., Pihlatie, M., Poulter, B., Rivas-Ubach, A., Schadt, C.W., Terazawa, K., Warner, D.L., Zhang, Z., Vargas, R., 2019. Methane emissions from tree stems: a new frontier in the global carbon cycle. New Phytol. 222, 18–28. https://doi.org/10.1111/nph.15582.

Bloemen, J., McGuire, M.A., Aubrey, D.P., Teskey, R.O., Steppe, K., 2013. Transport of root-respired CO_2 via the transpiration stream affects aboveground carbon assimilation and CO_2 efflux in trees. New Phytol. 197, 555–565. https://doi.org/10.1111/j.1469-8137.2012.04366.x.

Bréchet, L.M., Daniel, W., Stahl, C., Burban, B., Goret, J.-Y., Salomón, R.L., Janssens, I.A., 2021. Simultaneous tree stem and soil greenhouse gas (CO_2, CH_4, N_2O) flux measurements: a novel design for continuous monitoring towards improving flux estimates and temporal resolution. New Phytol. 230, 2487–2500. https://doi.org/10.1111/nph.17352.

Campioli, M., Malhi, Y., Vicca, S., Luyssaert, S., Papale, D., Peñuelas, J., Reichstein, M., Migliavacca, M., Arain, M.A., Janssens, I.A., 2016. Evaluating the convergence between eddy-covariance and biometric methods for assessing carbon budgets of forests. Nat. Commun. 7, 13717. https://doi.org/10.1038/ncomms13717.

CONAGUA – Comisión Nacional del Agua, 2023. Red de Estaciones Climatológicas Automáticas. Servicio Meteorológico Nacional. https://smn.conagua.gob.mx/es/ (accessed on 24th July 2023).

Covey, K.R., Megonigal, J.P., 2019. Methane production and emissions in trees and forests. New Phytol. 222, 35–51. https://doi.org/10.1111/nph.15624.

DMC – Dirección Meteorológica de Chile, 2023. Datos históricos de Estaciones Meteorológicas Automatizadas. Dirección General de Aeronáutica Civil. https://climatologia.meteochile.gob.cl/ (accessed on 24th July 2023).

Dušek, J., Nguyen, V.X., Le, T.X., Pavelka, M., 2021. Methane and carbon dioxide emissions from different ecosystems at the end of dry period in South Vietnam. Trop. Ecol. 62, 1–16. https://doi.org/10.1007/s42965-020-00118-1.

Epron, D., Mochidome, T., Tanabe, T., Dannoura, M., Sakabe, A., 2022. Variability in stem methane emissions and wood methane production of different tree species in a cold temperate mountain forest. Ecosystems. https://doi.org/10.1007/s10021-022-00795-0.

Flanagan, L.B., Nikkel, D.J., Scherloski, L.M., Tkach, R.E., Smits, K.M., Selinger, L.B., Rood, S.B., 2021. Multiple processes contribute to methane emission in a riparian cottonwood forest ecosystem. New Phytol. 229, 1970–1982. https://doi.org/10.1111/nph.16977.

Fraser-McDonald, A., Boardman, C., Gladding, T., Burnley, S., Gauci, V., 2022. Methane emissions from forested closed landfill sites: variations between tree species and landfill management practices. Sci. Total Environ. 838 (2) https://doi.org/10.1016/j.scitotenv.2022.156019.

Friedlingstein, P., Jones, M.W., O'Sullivan, M., Andrew, R.M., Bakker, D.C.E., Hauck, J., Le Quéré, C., Peters, G.P., Peters, W., Pongratz, J., Sitch, S., Canadell, J.G., Ciais, P., Jackson, R.B., Alin, S.R., Anthoni, P., Bates, N.R., Becker, M., Bellouin, Zeng, J., 2022. Global carbon budget 2021. Earth Syst. Sci. Data 14, 1917–2005. https://doi.org/10.5194/essd-14-1917-2022.

Gao, C.H., Zhang, S., Ding, Q.S., Wei, M.Y., Li, H., Li, J., Wen, C., Gao, G.F., Liu, Y., Zhou, J.J., Zhang, J.Y., You, Y.P., Zheng, H.L., 2021. Source or sink? A study on the methane flux from mangroves stems in Zhangjiang estuary, southeast coast of China. Sci. Total Environ. 788 https://doi.org/10.1016/j.scitotenv.2021.147782.

van Haren, J., Brewer, P.E., Kurtzberg, L., Wehr, R.N., Springer, V.L., Tello-Espinoza, R., Solignac-Ruiz, J., Cadillo-Quiroz, H., 2021. A versatile gas flux chamber reveals high tree stem CH_4 emissions in Amazonian peatland. Agric. For. Meteorol. 307, 108504 https://doi.org/10.1016/j.agrformet.2021.108504.

He, Y., Guan, W., Xue, D., Liu, L., Peng, C., Liao, B., Hu, J., Zhu, Q., Yang, Y., Wang, X., Zhou, G., Wu, Z., Chen, H., 2019. Comparison of methane emissions among invasive and native mangrove species in Dongzhaigang, Hainan Island. Sci. Total Environ. 697 https://doi.org/10.1016/j.scitotenv.2019.133945.

Hutchinson, G., Livingston, G., 2001. Vents and seals in non-steady-state chambers used for measuring gas exchange between soil and the atmosphere. Eur. J. Soil Sci. 52, 675–682. https://doi.org/10.1046/j.1365-2389.2001.00415.x.

Hutchinson, G.L., Mosier, A.R., 1981. Improved soil cover method for field measurement of nitrous oxide fluxes. Soil Sci. Soc. Am. J. 45, 311–316. https://doi.org/10.2136/sssaj1981.03615995004500020017x.

Jeffrey, L.C., Reithmaier, G., Sippo, J.Z., Johnston, S.G., Tait, D.R., Harada, Y., Maher, D. T., 2019. Are methane emissions from mangrove stems a cryptic carbon loss pathway? Insights from a catastrophic forest mortality. New Phytol. 224, 146–154. https://doi.org/10.1111/nph.15995.

Jeffrey, L.C., Maher, D.T., Tait, D.R., Johnston, S.G., 2020. A small nimble in situ fine-scale flux method for measuring tree stem greenhouse gas emissions and processes (S.N.I.F.F). Ecosystems 23, 1676–1689. https://doi.org/10.1007/s10021-020-00496-6.

Jeffrey, L.C., Maher, D.T., Tait, D.R., Reading, M.J., Chiri, E., Greening, C., Johnston, S. G., 2021. Isotopic evidence for axial tree stem methane oxidation within subtropical lowland forests. New Phytol. 230, 2200–2212. https://doi.org/10.1111/nph.17343.

Jiang, J., Hu, J., Xu, X., Li, Y., Sheng, J., 2023. Effect of near-surface winds on the measurement of forest soil CO_2 fluxes using closed air chambers. Front. Ecol. Evol. 11, 1163704. https://doi.org/10.3389/fevo.2023.1163704.

Juszczak, R., 2013. Biases in methane chamber measurements in peatlands. Int. Agrophys. 27 (2), 159–168. https://doi.org/10.2478/V10247-012-0081-Z.

Kohl, L., Koskinen, M., Polvinen, T., Tenhovirta, S., Rissanen, K., Patama, M., Zanetti, A., Pihlatie, M., 2021. An automated system for trace gas flux measurements from plant foliage and other plant compartments. Atmos. Meas. Tech. 14, 4445–4460. https://doi.org/10.5194/amt-14-4445-2021.

Kutzbach, L., Schneider, J., Sachs, T., Giebels, M., Nykänen, H., Shurpali, N.J., Martikainen, P.J., Alm, J., Wilmking, M., 2007. CO_2 flux determination by closed-chamber methods can be seriously biased by inappropriate application of linear regression. Biogeosciences 4 (6), 1005–1025. https://doi.org/10.5194/BG-4-1005-2007.

Machacova, K., Warlo, H., Svobodová, K., Agyei, T., Uchytilová, T., Horáček, P., Lang, F., 2023. Methane emission from stems of European beech (*Fagus sylvatica*) offsets as much as half of methane oxidation in soil. New Phytol. 238, 584–597. https://doi.org/10.1111/nph.18726.

Maier, M., Mayer, S., Laemmel, T., 2019. Rain and wind affect chamber measurements. Agric. For. Meteorol. 279 https://doi.org/10.1016/j.agrformet.2019.107754.

Orellana, R., Espadas, C., Conde, C., Gay, C., 2010. Atlas: Escenarios de cambio climático en la Península de Yucatán. Centro de Investigación Científica de Yucatán A.C, México (111 pp.).

OriginLab Corporation, 2016. Origin(Pro), Version Number 2016. Northampton, MA, USA. https://www.originlab.com/.

Pangala, S.R., Enrich-Prast, A., Basso, L.S., Peixoto, R.B., Bastviken, D., Hornibrook, E.R. C., Gatti, L.V., Marotta, H., Calazans, L.S.B., Sakuragui, C.M., Bastos, W.R., Malm, O., Gloor, E., Miller, J.B., Gauci, V., 2017. Large emissions from floodplain trees close the Amazon methane budget. Nature 552, 230–234. https://doi.org/10.1038/nature24639.

Pedersen, A.R., Petersen, S.O., Schelde, K., 2010. A comprehensive approach to soil-atmosphere trace-gas flux estimation with static chambers. Eur. J. Soil Sci. 61 (6), 888–902. https://doi.org/10.1111/j.1365-2389.2010.01291.x.

Pihlatie, M.K., Christiansen, J.R., Aaltonen, H., Korhonen, J.F.J., Nordbo, A., Rasilo, T., Benanti, G., Giebels, M., Helmy, M., Sheehy, J., Jones, S., Juszczak, R., Klefoth, R., Lobo-do-Vale, R., Rosa, A.P., Schreiber, P., Serça, D., Vicca, S., Wolf, B., Pumpanen, J., 2013. Comparison of static chambers to measure CH_4 emissions from soils. Agric. For. Meteorol. 171-172, 124–136. https://doi.org/10.1016/j.agrformet.2012.11.008.

Pitz, S., Megonigal, J.P., 2017. Temperate forest methane sink diminished by tree emissions. New Phytol. 214 (4), 1432–1439. https://doi.org/10.1111/nph.14559.

Posit Team, 2023. RStudio: Integrated Development Environment for R. Posit Software, PBC, Boston, MA. URL. http://www.posit.co/.

Salomón, R.L., Rodríguez-Calcerrada, J., Staudt, M., 2017. Carbon losses from respiration and emission of volatile organic compounds – the overlooked side of tree carbon budgets. In: Gil-Pelegrín, E., Peguero-Pina, J.J., Sancho-Knapik, D. (Eds.), Oaks Physiological Ecology. Exploring the Functional Diversity of Genus Quercus L. Springer International, Cham, Switzerland, pp. 327–359. https://doi.org/10.1007/978-3-319-69099-5_10.

Saunois, M., Stavert, A.R., Poulter, B., Bousquet, P., Canadell, J.G., Jackson, R.B., Raymond, P.A., Dlugokencky, E.J., Houweling, S., Patra, P.K., Ciais, P., Arora, V.K., Bastviken, D., Bergamaschi, P., Blake, D.R., Brailsford, G., Bruhwiler, L., Carlson, K. M., Carrol, M., Zhuang, Q., 2020. The global methane budget 2000–2017. Earth Syst. Sci. Data 12 (3), 1561–1623. https://doi.org/10.5194/essd-12-1561-2020.

Schneider, C., Rasband, W., Eliceiri, K., 2012. NIH image to ImageJ: 25 years of image analysis. Nat. Methods 9, 671–675. https://doi.org/10.1038/nmeth.2089.

Siegenthaler, A., Welch, B., Pangala, S.R., Peacock, M., Gauci, V., 2016. Technical note: semi-rigid chambers for methane gas flux measurements on tree stems. Biogeosciences 13, 1197–1207. https://doi.org/10.5194/bg-13-1197-2016.

Teskey, R.O., Saveyn, A., Steppe, K., McGuire, M.A., 2008. Origin, fate and significance of CO_2 in tree stems. New Phytol. 177, 17–32. https://doi.org/10.1111/j.1469-8137.2007.02286.x.

Teskey, R.O., McGuire, A., Bloemen, J., Aubrey, D.P., Steppe, K., 2017. Respiration and CO_2 fluxes in trees. In: Tcherkez, G., Ghashghaie, J. (Eds.), Plant Respiration: Metabolic Fluxes and Carbon Balance, Advances in Photosynthesis and Respiration 43. Springer, Cham, Switzerland, pp. 181–207. https://doi.org/10.1007/978-3-319-68703-2_9.

Vroom, R.J.E., van den Berg, M., Pangala, S.R., van der Scheer, O.E., Sorrell, B.K., 2022. Physiological processes affecting methane transport by wetland vegetation – a review. Aquat. Bot. 182 https://doi.org/10.1016/j.aquabot.2022.103547.

Welles, J.M., Demetriades-Shah, T.H., McDermitt, D.K., 2001. Considerations for measuring ground CO_2 effluxes with chambers. Chem. Geol. 177 (1–2), 3–13. https://doi.org/10.1016/s0009-2541(00)00388-0.

Wilkinson, J., Bors, C., Burgis, F., Lorke, A., Bodmer, P., 2018. Measuring CO_2 and CH_4 with a portable gas analyzer: closed-loop operation, optimization and assessment. PLoS One 13 (4), e0193973. https://doi.org/10.1371/journal.pone.0193973.

Xiao, S., Wang, C., Wilkinson, R.J., Liu, D., Zhang, C., Xu, W., Yang, Z., Wang, Y., Lei, D., 2016. Theoretical model for diffusive greenhouse gas fluxes estimation across water-

air interfaces measured with the static floating chamber method. Atmos. Environ. 137, 45–52. https://doi.org/10.1016/j.atmosenv.2016.04.036.
Yáñez-Espinosa, L., Ángeles, G., 2022. Does mangrove stem bark have an internal pathway for gas flow? Trees 36, 361–377. https://doi.org/10.1007/s00468-021-02210-y.
Yang, J., He, Y., Aubrey, D.P., Zhuang, Q., Teskey, R.O., 2016. Global patterns and predictors of stem CO_2 efflux in forest ecosystems. Glob. Chang. Biol. 22, 1433–1444. https://doi.org/10.1111/gcb.13188.
Zhang, Y.X., Huang, J.F., Luo, M., Wu, Z., Li, H., Chen, K.L., Tan, J., 2019. Rate of methane transport and respiration from the stem of mangrove *Kandelia obovata* at different part of intertidal zone in Zhangjiang river estuary. Res. Environ. Sci. 32 (5), 839–847. https://doi.org/10.13198/j.issn.1001-6929.2018.09.14.